0022-3565/10/3322-650–658$20.00
THE JOURNAL OF PHARMACOLOGY AND EXPERIMENTAL THERAPEUTICS
JPET 332:650–658, 2010

Vol. 332, No. 2
160515/3551563
Printed in U.S.A.

Putative Transmembrane Domain 12 of the Human Organic Anion Transporter hOAT1 Determines Transporter Stability and Maturation Efficiency

Mei Hong, Shanshan Li, Fanfan Zhou, Paul E. Thomas, and Guofeng You

Departments of Pharmaceutics (M.H., S.L., F.Z., G.Y.) and Toxicology (P.E.T.), Rutgers, the State University of New Jersey, Piscataway, New Jersey; and Department of Pharmacology, University of Medicine and Dentistry of New Jersey-Robert Wood Johnson Medical School, Piscataway, New Jersey (G.Y.)

Received August 14, 2009; accepted October 16, 2009

ABSTRACT

Human organic anion transporter hOAT1 plays a critical role in the body disposition of clinically important drugs. In transmembrane segment (TM) 12, residues Tyr-490 and dileucine Leu-503/Leu-504 were identified to be critical for hOAT1 function. Substitution of Tyr-490 with alanine led to a dramatic reduction in protein expression of hOAT1 and its transport activity. The contribution of the side chain of Tyr-490 to transport activity was then evaluated by replacing this residue with Trp or Phe. Substitution of Tyr-490 with Trp or Phe partially or fully recovered the protein expression of hOAT1 and its transport activity, respectively, that were lost by substitution of Tyr-490 with alanine, suggesting that the aromatic ring and the size of the side chain of Tyr-490 are critical for hOAT1 expression and function. Studies with protease inhibitors and pulse-chase labeling further showed that the loss of expression of hOAT1 and its transport activity by replacing Tyr-490 with alanine resulted from accelerated degradation of the transporter, whereas its maturation efficiency was not affected. In contrast to Tyr-490, substitution of Leu-503/Leu-504 with alanine also resulted in complete loss of protein expression of hOAT1 and its transport activity. However, such loss of protein expression could not be prevented by treating mutant-expressing cells with protease inhibitors. Pulse-chase experiments showed that the mutant transporter (L503/L504A) was trapped in the endoplasmic reticulum without conversion into mature form of the transporter. Our results are the first to highlight the central role of TM 12 in maintaining the stability and in promoting the maturation efficiency of hOAT1.

The organic anion transporter family (OAT) belongs to the amphiphilic solute carrier transporters family 22a (SLC22A), which transports a broad diversity of substrates including metabolites, toxins, and clinical drugs such as β-lactam antibiotics, antivirals, angiotensin-converting enzyme inhibitors, diuretics, and nonsteroidal anti-inflammatory drugs (You, 2004; Anzai et al., 2006; El-Sheikh et al., 2008; Srimaroeng et al., 2008). To date, ten members of the OAT family (OAT1–10) have been identified (Sekine et al., 1997, 1998; Sweet et al., 1997; Kusuhara et al., 1999; Cha et al., 2000; Youngblood and Sweet, 2004; Schnabolk et al., 2006; Shin et al., 2007; Bahn et al., 2008; Yokoyama et al., 2008), which differ from each other by their localization, expression level, and substrate specificity.

In the kidney, OAT1 and OAT3 use a tertiary transport mechanism to move organic anions across the basolateral membrane into the proximal tubule cells for subsequent exit across the apical membrane into the urine for elimination (You, 2004; Anzai et al., 2006; El-Sheikh et al., 2008; Srimaroeng et al., 2008). Through this tertiary transport mechanism, Na^+K^+-ATPase maintains an inwardly directed (blood-to-cell) Na^+ gradient. The Na^+ gradient then drives a sodium dicarboxylate cotransporter, sustaining an outwardly directed dicarboxylate gradient that is used by a dicarboxylate/organic anion exchanger to move the organic anion substrate into the cell. This cascade of events indirectly links organic anion transport to metabolic energy and the Na^+ gradient, allowing the entry of a negatively charged substrate against both its chemical concentration gradient and the electrical potential of the cell.

This work was supported by the National Institutes of Health National Institute of Diabetes Digestive and Kidney Diseases [Grant R01-DK061652] (to G.Y,); and the National Institutes of Health National Institute of General Medical Sciences [Grant R01-GM079123] (to G.Y.).

M.H. and S.L. contributed equally to this work.

Article, publication date, and citation information can be found at http://jpet.aspetjournals.org.
doi:10.1124/jpet.109.160515.

ABBREVIATIONS: OAT, organic anion transporter; OCT, organic cation transporter; PAH, *p*-aminohippurate; PBS, phosphate-buffered saline; PAGE, polyacrylamide gel electrophoresis; DMEM, Dulbecco's modified Eagle's medium; ER, endoplasmic reticulum; Wt, wild type; MFS, major facilitator superfamily; TM, transmembrane segment; MG132, *N*-benzoyloxycarbonyl (*Z*)-Leu-Leu-leucinal.

Despite the clinical importance of these transporters, much remains to be understood regarding the contribution of OAT structure to their transport activity and regulation. All of the cloned OATs share several common structural features including 12 transmembrane domains flanked by intracellular N and C termini; multiple glycosylation sites localized in the first extracellular loop between transmembrane domains 1 and 2, and multiple potential phosphorylation sites present in the intracellular loop between transmembrane domains 6 and 7, and in the C terminus. Investigation from our laboratory on the structure-function relationship of OATs revealed that glycosylation is necessary for the targeting of these transporters to the plasma membrane (Tanaka et al., 2004; Zhou et al., 2005). We also showed that the first transmembrane domain of hOAT1 plays an important role in both the targeting of the transporter to the cell surface and its substrate recognition (Hong et al., 2004). Previously, Bahn et al. (2004) reported the existence of several alternative splice variants of hOAT1 in the kidney. The functional characterization of these variants revealed that two such variants, hOAT1-3 and hOAT1-4, both of which possess a deletion of TM 11 and TM 12 exhibited no transport activity. Their results prompted us to hypothesize that TM 11 and/or TM 12 may play a critical role in hOAT1 function. In the present study, we investigated the importance of TM 12 in hOAT1. We identified several amino acids critically involved in hOAT1 function.

Materials and Methods

p-[^{3}H]Aminohippuric acid (PAH) was from PerkinElmer Life and Analytical Sciences (Waltham, MA). Membrane-impermeable biotinylation reagent NHS-SS-biotin and streptavidin agarose beads were purchased from Pierce Chemcial (Rockford, IL). Rec-Protein G Sepharose 4B beads were purchased from Invitrogen (Carlsbad, CA). QuickChange site-directed mutagenesis kits were purchased from Stratagene (La Jolla, CA). COS-7 cells and LLC-PK1 cells were purchased from American Type Culture Collection (Manassas, VA). All other reagents were purchased from Sigma-Aldrich (St. Louis, MO).

Site-Directed Mutagenesis. Mutant transporters were generated by site-directed mutagenesis by use of hOAT1 or hOAT1-*myc* as a template. hOAT1-*myc* contains a 10-amino-acid c-*myc* tag at the C terminus of hOAT1. Previous studies from our laboratory (Tanaka et al., 2004) showed that the *myc*-tagged protein retained the functional properties of the native (unmodified) structure. The mutant sequences were confirmed by the dideoxy chain termination method.

Cell Culture and Transfections. COS-7 cells were grown in Dulbecco's modified Eagle's medium containing 10% fetal bovine serum and antibiotics. LLC-PK1 cells were grown in Medium 199 containing 10% fetal bovine serum. Cells were grown to 90 to 100% confluence and transfected with the appropriate plasmids by use of Lipofectamine 2000 (Invitrogen).

Transport Measurements. For each well, uptake solution was added. The uptake solution consisted of phosphate-buffered saline (PBS)/CM (137 mM NaCl, 2.7 mM KCl, 4.3 mM Na_2HPO_4, 1.4 mM KH_2PO_4, 0.1 mM $CaCl_2$, and 1 mM $MgCl_2$, pH 7.3) and [^{3}H]PAH (20 μM). At the times indicated in the figure legends, the uptake was stopped by aspirating the uptake solution off and rapidly washing the cells with ice-cold PBS solution. The cells were then solubilized in 0.2 N NaOH, neutralized in 0.2 N HCl, and aliquoted for liquid scintillation counting. The uptake count was standardized by the amount of protein in each well.

Cell Surface Biotinylation. Cell surface expression levels of hOAT1 and its mutants were examined by use of the membrane-impermeable biotinylation reagent, NHS-SS-biotin (Pierce Chemical). hOAT1 and its mutants were expressed in cells grown in 6-well plates by use of Lipofectamine 2000 as described above. After 48 h, the medium was removed and the cells were washed twice with 3 ml of ice-cold PBS/CM, pH 8.0. The plates were kept on ice and all solutions were ice-cold for the rest of the procedure. Each well of cells was incubated with 1 ml of NHS-SS-biotin (0.5 mg/ml in PBS/CM) in two successive 20-min incubations on ice with very gentle shaking. The reagent was freshly prepared for each incubation. After biotinylation, each well was rinsed briefly with 3 ml of PBS/CM containing 100 mM glycine, then incubated with the same solution for 20 min on ice, to ensure complete quenching of the unreacted NHS-SS-biotin. The cells were then dissolved on ice for 1 h in 400 μl of lysis buffer (10 mM Tris, 150 mM NaCl, 1 mM EDTA, 0.1% SDS, 1% Triton X-100 with 1:100 protease inhibitor cocktail (Sigma-Aldrich). The cell lysates were cleared by centrifugation at 16,000*g* at 4°C. Fifty microliters of streptavidin-agarose beads (Pierce Chemical) were then added to the supernatant to isolate cell membrane protein. hOAT1 and its mutants were detected in the pool of surface proteins by SDS-PAGE and immunoblotting.

Metabolic Labeling and Immunoprecipitation. LLC-PK1 cells expressing hOAT1 and its mutants were washed twice with PBS and incubated for 45 min in methionine-free DMEM at 37°C and 5% CO_2. Radiolabeling of cell proteins was carried out by replacing the medium with fresh methionine-free DMEM supplemented with 100 μCi [^{35}S]methionine and incubated for 30 min at 37°C and 5% CO_2. The chase was started by aspirating the [^{35}S]methionine-containing medium, followed by two PBS washes and incubation in the complete DMEM containing 10% fetal calf serum for different time periods. The labeled cells were then washed twice with PBS and harvested for lysate preparation with use of 400 μl of lysis buffer. The cell lysates were cleared by centrifugation at 16,000*g* for 30 min at 4°C. The supernatants were then precleaned with 30 μl of Protein G beads to reduce nonspecific binding. The precleaned cell lysates (~400 μl) were incubated with 4 μg of anti-*myc* antibody for overnight at 4°C. Thirty microliters of Protein G beads were then added and mixed with end-over-end rotating at 4°C for 3 h. Proteins bound to the Protein G beads were denatured in Laemmli buffer for SDS-PAGE and autoradiography.

Protease Treatment. hOAT1 and its mutants were transfected into LLC-PK1 cells grown in 12-well plates by use of Lipofectamine 2000. Cells were then incubated in DMEM containing proteasome inhibitors MG132 (10 μM), lactacystin (10 μM), or lysosomal inhibitors leupeptin/pepstatinA (50, 100 μg/ml), NH_4Cl (2, 5, 15 mM), and chloroquine (100, 200 μM) individually. Treated cells were collected at specific time points as indicated in the figure legends and lysed. Equal amount of proteins were loaded on 7.5% SDS-PAGE minigels and analyzed by immunoblotting as described earlier.

Electrophoresis and Immunoblotting. Protein samples (100 μg) were resolved on 7.5% SDS-PAGE minigels and electroblotted on to polyvinylidene difluoride membranes. The blots were blocked for 1 h with 5% nonfat dry milk in PBS-0.05% Tween 20, washed, and incubated for 1 h at room temperature with appropriate primary antibodies followed by horseradish peroxidase-conjugated secondary antibodies. The signals were detected by SuperSignal West Dura Extended Duration Substrate kit (Pierce Chemical). Nonsaturating, immunoreactive protein bands were quantified by scanning densitometry with FluorChem 8000 imaging system (Alpha Innotech, San Leandro, CA).

Data Analysis. Data were analyzed for statistical significance by use of one-way ANOVA analysis or Student's *t* test. Differences with p values of <0.05 were considered statistically significant.

Results

Alanine Scanning of Residues in TM 12. To probe the contribution of each residue in TM 12 to hOAT1 function, we systematically replaced each residue with alanine (A) by use

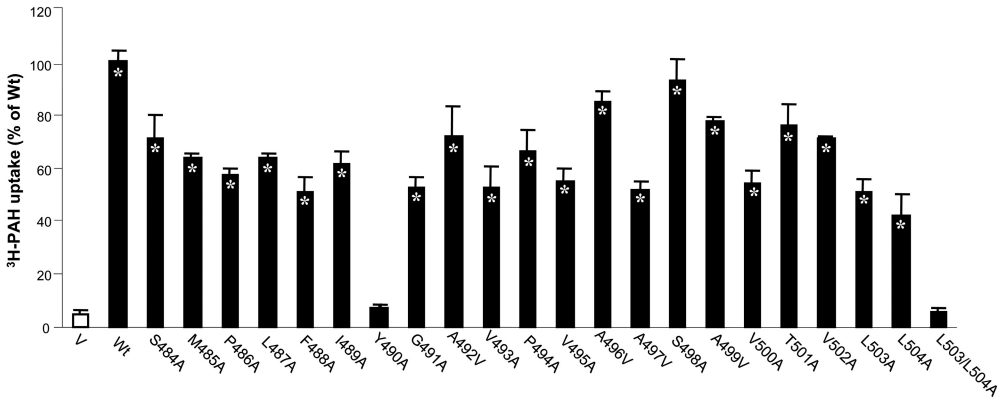

Fig. 1. ^{3}H-labeled PAH uptake by hOAT1 wild type (Wt) and its alanine-substituted mutants. The mutants were generated by use of hOAT1-*myc* as template. Transport of PAH (20 μM, 3 min) in COS-7 cells expressing hOAT1 Wt and its alanine-substituted mutants was measured. Uptake activity was expressed as a percentage of the uptake measured in Wt. The results represent data from three experiments, with triplicate measurements for each mutant. *, values significantly different ($p < 0.05$) from that of pcDNA vector (V, mock control). The uptake in LLC-PK1 cells gave similar results (not shown).

of hOAT1-*myc* as template. Because of the multiple roles of dileucine motif (LL) plays in other transporters (Bello et al., 2001; Peña-Münzenmayer et al., 2005; Eckhardt et al., 2006), the double mutant L503/L504A was also generated. The functional properties of these mutants were then determined by measuring the uptake of [^{3}H]PAH in mutant-transfected cells. Results obtained from this analysis are shown in Fig. 1. Although most of the mutants exhibited significant transport activities compared with hOAT1 wild type, mutants Y490A and L503/L504A almost completely lost transport activity. Mutants Y490A and L503/L504A were also generated by use of untagged hOAT1 as template, and the similar results were obtained (data not shown). Wild-type hOAT1 functions as an organic anion exchanger with one anion being transported into the cells in exchange for another anion being effluxed out of the cells. Wild-type hOAT1 is also sensitive to the inhibition by probenecid. Our efflux experiment and inhibition study revealed that all the active mutants retained the characteristic of hOAT1 wild type as an organic anion exchanger and with sensitivity to inhibition by probenecid (data not shown). Because of the loss in the uptake of PAH by Y490A and L503/L504A, additional studies were focused on these mutants.

The Role of Tyr-490 in hOAT1 Function. To further evaluate the role of Tyr-490 in hOAT1 function, we mutagenized Tyr-490 to two other aromatic residues Phe and Trp. As shown in Fig. 2a, substitution of Tyr-490 with Trp (the resulting mutant Y490W) partially recovered the transport activity lost by substitution with alanine, whereas substitution of Tyr-490 with Phe (the resulting mutant Y490F) almost completely recovered the transport activity. Such pattern of uptake was observed in both COS-7 cells and in LLC-PK1 cells. Kinetic analysis of Y490W (Fig. 2, b and c) showed that the decreased transport activity of this mutant mainly resulted from a decreased V_{max} (V_{max}, 0.037 ± 0.004 pmol/μg every 3 min with wild-type hOAT1, and 0.021 ± 0.005 pmol/μg every 3 min with Y490W) without significant change in K_m (K_m, 16.7 ± 0.7 μM for wild-type hOAT1 and 15.9 ± 0.6 μM for Y490W). Because cellular uptake of PAH requires that the transporter be localized to the plasma membrane, we tested by immunoblot analysis whether the reduced or the abolished transport activity was caused by ab-

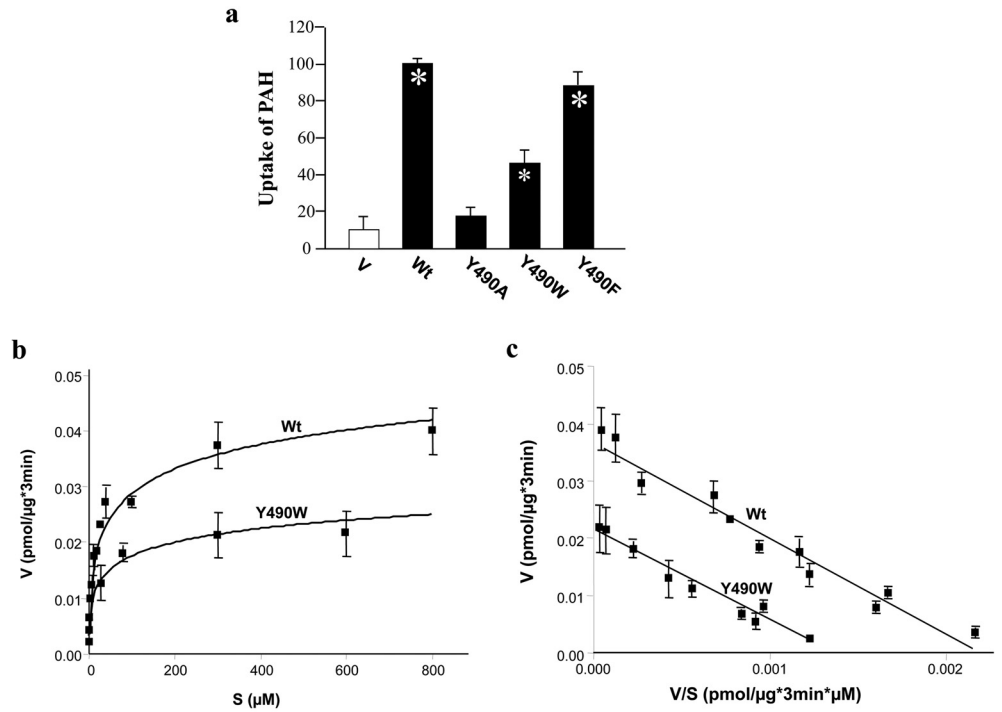

Fig. 2. Effects of mutation at Tyr-490 on hOAT1 function. a, effects of mutation at Tyr-490 on the function of hOAT1. ^{3}H-Labeled PAH uptake (20 μM, 3 min) was measured in cells expressing hOAT1 wild-type (Wt), pcDNA vector (V, mock control), Y490A, Y490W, and Y490F. The results represent data from three experiments, with triplicate measurements for each mutant. *, values significantly different ($p < 0.05$) from that of mock control (V). b, kinetic analysis of PAH transport mediated by hOAT1 Wt and mutant Y490W. Kinetic characteristics were determined at the initial rate of uptake (3-min uptake) with substrate concentration ranging from 2 to 800 μM in cells expressing hOAT1Wt, mutant Y490W, or pcDNA vector (mock control). The data represent uptake into hOAT1 Wt-, hOAT1 mutant Y490W-transfected cells minus uptake into pcDNA vector-transfected cells. Values are mean ± S.E. ($n = 3$). c, transport kinetic values were calculated by use of the Eadie-Hofstee transformation. V, velocity; S, substrate concentration. Values were mean of three experiments, and the error bars show the range of observations.

normal expression of the transporter on the cell surface and in the total cell extracts. As shown in Fig. 3a (top), cell surface expression of Y490A dramatically decreased. In total cell lysates (Fig. 3a, bottom), the transporter runs as two bands of 60 (shown as arrowhead) and 80 (shown as arrow) kDa apparent sizes. We previously showed (Tanaka et al., 2004; Zhou et al., 2005) that the lower band was sensitive to the treatment of endoglyosidase H, and therefore corresponds to core-glycosylated immature form of the protein, which resides in the endoplasmic reticulum (ER). The upper band was resistant to the treatment of endoglyosidase H, and therefore corresponds to the fully processed and glycosylated mature form of the protein, which is expressed at the cell surface. The low level of the immature band compared with the high level of the mature band indicates the high maturation efficiency of the transporter in these cells. The total expression of Y490A (both the mature and the immature form) was also decreased dramatically (Fig. 3a, bottom). The expression of the mutants correlated well with their functional activity. Mutant Y490F had expression similar to that of the wild-type hOAT1. Y490W had moderate expression, whereas the expression of Y490A was undetectable. The lack of the expression of the transporter when Tyr-490 was substituted by alanine could result from the decreased protein synthesis or accelerated degradation. To investigate the underlying mechanisms, we used a battery of protease inhibitors. Cells degrade proteins through two major systems, the proteasome and the lysosome. The proteasome is involved in the degradation of most cytosolic and nuclear proteins and some membrane proteins (Jensen et al., 1995; Sepp-Lorenzino et al., 1995; Ward et al., 1995) and removes misfolded or misaggregated proteins in the endoplasmic reticulum (Kopito, 1997). The lysosome degrades membrane proteins and extracellular materials that enter the cell via endocytosis (Ward et al., 1995). These different pathways of proteolysis can be determined by their sensitivity to different inhibitors. Degradation of polypeptides by the proteasome can be inhibited by MG132 and lactacystin. Lysosomal proteolysis can be inhibited by leupeptin, pepstatin A, ammonium chloride (NH_4Cl), or chloroquine. As shown in Fig. 4, treatment of cells expressing wild-type hOAT1 and mutant Y490A with lysosomal inhibitors led to the accumulation of the mature form (80 kDa) for both the wild type and its mutant in the total cell lysates (Fig. 4a). Further studies through cell surface biotinylation and functional analysis showed that the increased mature form in the total cell lysate was accompanied by an increase of Y490A at the cell surface (Fig. 4c), as a consequence, resulting in an increased transport activity (Fig. 4e). Treatment of cells with proteasomal inhibitors MG132 (Fig. 5a) and lactacystin (Fig. 5c) resulted in the accumulation of a nonglycosylated form (47 kDa), a partially glycosylated immature form (60 kDa), a fully glycosylated cell mature form (80 kDa), and some high-molecular-mass band for both the wild type and its mutant in the total cell lysates. These OAT1-immunoreactive bands are MG132-, and lactacystin-specific, because they were not observed in the absence of the inhibitors. The high-molecular-mass band may result from the aggregation of the immature form and was also observed in other transporters when treated with the proteasomal inhibitors (Bauman and Blakely, 2002). However, cell surface biotinylation study showed that the increased mature form of Y490A in the total cell lysates by MG-132 and lactacystin treatments did not result in any detectable cell surface expression of this mutant (not shown). The effect of Y490A on the maturation efficiency of the transporter was then examined by pulse-chase experiments (Fig. 6). The newly synthesized proteins were pulse-labeled with ^{35}[S]methionine and chased for different time periods. After 2 h of chasing, significant amount of immature form (shown as arrow head) of hOAT1 wild-type (Wt) and mutant Y490A was converted to mature form (shown as arrow). Therefore, mutant Y490A had a maturation efficiency similar to that of the wild type.

The Role of L503/L504 in hOAT1 Function. Similar to Y490A, substitution of L503/L504 with alanine also resulted in an abolished transport activity because of the loss of the expression of the transporter both at the cell surface (Fig. 7a) and in the total cell lysates (both the mature form and the immature form) (Fig. 7b). However, in contrast to Y490A, treatment of cells expressing L503/L504A with lysosomal inhibitors did not lead to the accumulation of either the mature form (80 kDa), or the immature form of the transporter in the total cell lysates (Fig. 8). Treatment of the cells with proteasomal inhibitors MG132 or lactacystin only re-

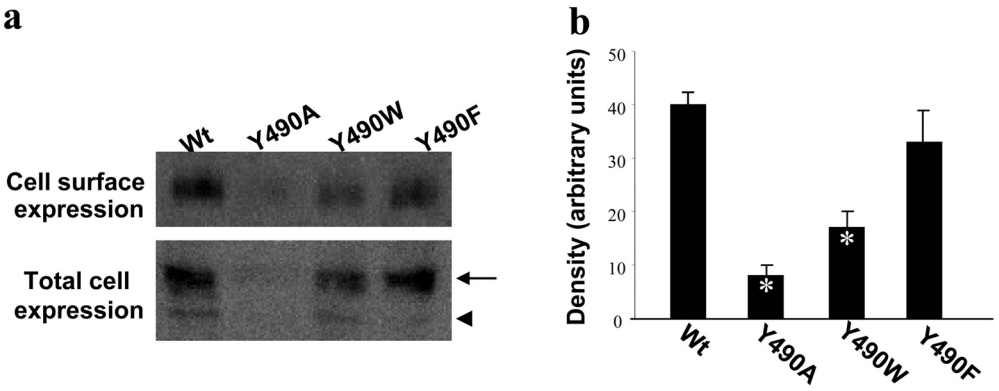

Fig. 3. Effects of mutations at Tyr-490 on cell surface and total cell expression of hOAT1. a (top), Western blot analysis of cell surface expression of hOAT1 Wt and its mutants. Cells were biotinylated, and the labeled cell surface proteins were precipitated with streptavidin beads, separated by SDS-PAGE, followed by Western blotting with anti-*myc* antibody (1:100). (bottom) Total cell expression of hOAT1 Wt and its mutants. Cells were lysed, and their proteins were separated by SDS-PAGE, followed by Western blotting with anti-*myc* antibody. Mature form was shown as arrow and immature form was shown as arrowhead. b, densitometry analysis of cell surface expression of Y490 mutants shown in a (top). *, values significantly different ($p < 0.05$) from that of Wt.

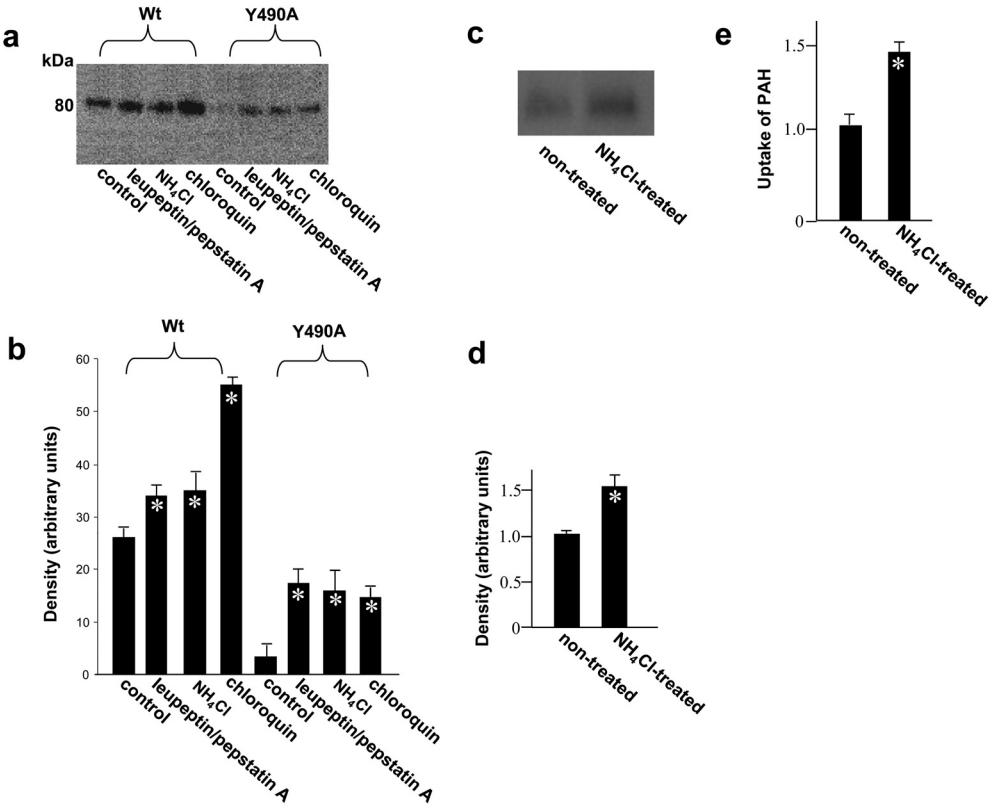

Fig. 4. Effect of lysosomal inhibitors on Wt hOAT1 and its mutant Y490A. a, Western blot analysis of total cell expression of hOAT1 Wt and Y490A in cells treated with or without lysosomal inhibitors. Cells were treated for 16 h with or without lysosomal inhibitors leupeptin/pepstatin A (50 μg/ml), NH_4Cl (2 mM), and chloroquin (100 μM). Treated cells were then lysed, followed by Western blotting using anti-*myc* antibody (1:100). b, densitometry analysis of band densities from a. The results represent data from three experiments. c, cell surface expression of Y490A in cells treated with or without lysosomal inhibitor NH_4Cl. Cells were treated for 16 h with or without lysosomal inhibitor NH_4Cl (2 mM), followed by cell surface biotinylation and Western blotting with use of anti-*myc* antibody (1:100). d, densitometry analysis of band densities from c. The results represent data from three experiments. ∗, values significantly different ($p < 0.05$) from that of the density measured in Y490A-expressing cells treated without NH_4Cl. e, ^3H-labeled PAH uptake in Y490A-expressing cells treated with or without lysosomal inhibitor NH_4Cl. Uptake activity was expressed as a percentage of the uptake measured in Y490A-expressing cells treated without NH_4Cl. The results represent data from three experiments, with triplicate measurements for each mutant. ∗, values significantly different ($p < 0.05$) from that of the uptake measured in Y490A-expressing cells treated without NH_4Cl.

sulted in the accumulation of small amount of a partially glycosylated form (60 kDa) of the mutant transporter (Fig. 9) in the total cell lysate. The inability of these protease inhibitors to accumulate the mature form of L503/L504A suggests that accelerated degradation may not be the main mechanism for the lack of mature form of this mutant. To determine whether the lack in the mature form of this mutant reflects decreased maturation efficiency, we again performed pulse-chase experiments (Fig. 10). After 2 h of chasing, significant amount of immature form (shown as arrow head) of hOAT1 Wt was converted to mature form (shown as arrow). In contrast, the conversion of the immature form of mutant L503/L504A to mature form never occurred, suggesting that L503/L504 is critical for the maturation of the transporter. However, the lack of maturation of L503/L504A could be due to the alteration of the specific dileucine, or to the simultaneous alteration of two amino acids at a specific location. To differentiate between these possibilities, we constructed a different double mutant of Leu-503 with another adjacent residue Val-502. Our results (Fig. 11) showed that the mutant V502/L503A exhibited significant transport activity indicating that mutation at V502/L503 did not prevent the transporter from producing a fully glycosylated cell surface form of the transporter. These results suggest that it is the dileucine rather than the specific location of L503/L504 that has a specific role in promoting the maturation of hOAT1.

Discussion

OAT family and another closely related organic cation transporter OCT family belong to a large group of related proteins, the major facilitator superfamily (MFS). The members of MFS share common structural features, including 12 putative transmembrane-spanning domains and intracellular carboxyl and amino termini. The elucidation of high-resolution crystal structures of two other MFS members, LacY (Abramson et al., 2003) and GlpT (Huang et al., 2003), suggests that all MFS members may share a common fold. Based on such assumption, three-dimensional structure models of rat OCT1, rabbit OCT2, and human OAT1 have been developed by use of the template structure of LacY and GlpT (Popp et al., 2005, Zhang et al., 2005, Perry et al., 2006). In these models, transmembrane domains 1, 2, 4, 5, 7, 8, 10, and 11 form a large hydrophilic cleft for substrate binding, whereas other transmembrane domains such as transmembrane domain 12 (TM 12) were thought to provide support for the transporter. In the current studies, the important role of TM 12 has been revealed. This information may improve our

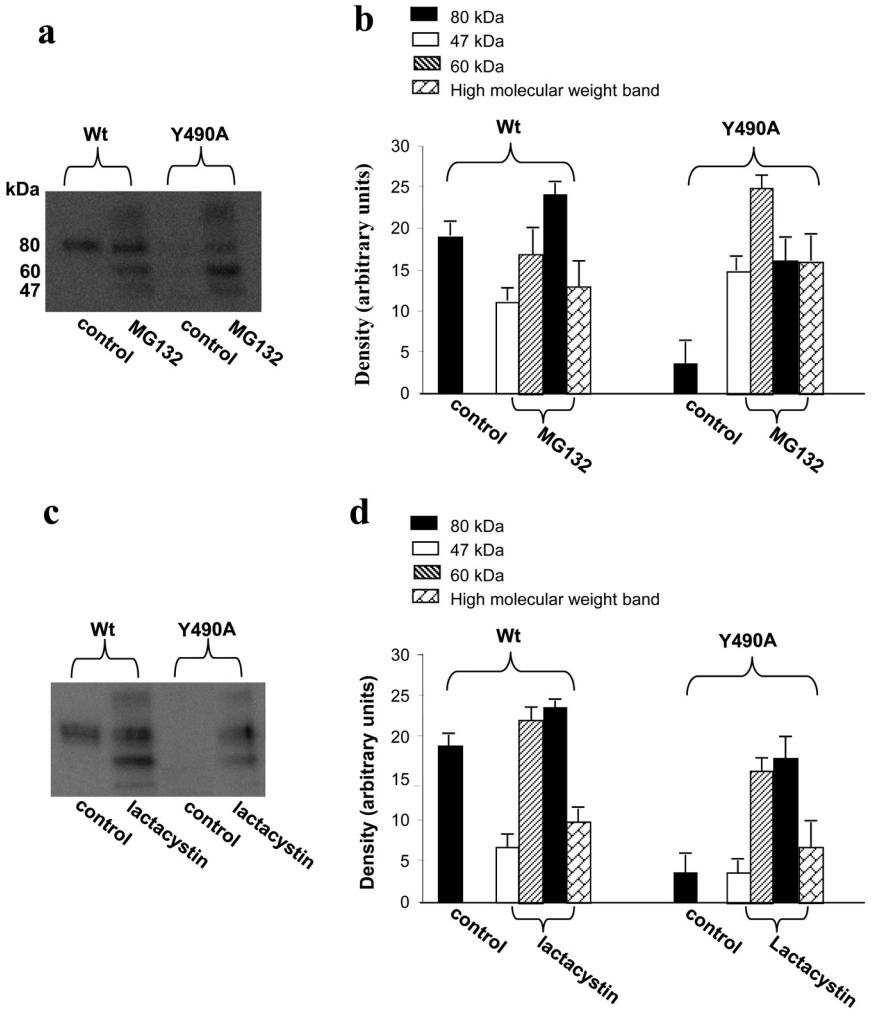

Fig. 5. Effect of proteasomal inhibitors on Wt hOAT1 and its mutant Y490A. a, c, Western blot analysis of total cell expression of hOAT1 Wt and Y490A in cells treated with or without proteasomal inhibitors. Cells were treated for 6 h with or without proteasomal inhibitors MG132 (10 μM) (a) or lactacystin (10 μM) (c). Treated cells were then lysed, followed by Western blotting with anti-*myc* antibody (1:100). b, d, densitometry analysis of band densities from a and c as well as other experiments. The results represent data from three experiments.

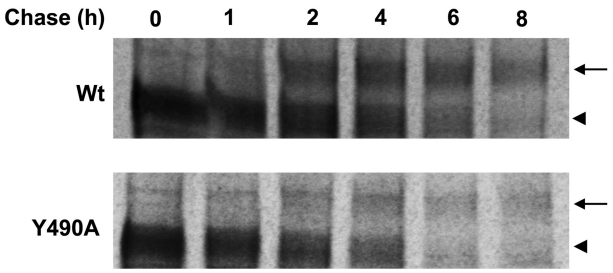

Fig. 6. Pulse-chase analyses of the role of Y490 in the maturation of hOAT1. The chase began after 30 min of pulse labeling. Mature form was shown as arrow, and immature form was shown as arrowhead.

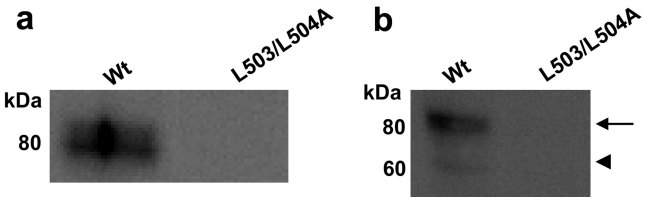

Fig. 7. Cell surface and total cell expression of hOAT1 Wt and its mutant L503A/L504A. a, Western blot analysis of cell surface expression of hOAT1 Wt and its mutant L503A/L504A. Cells were biotinylated, and the labeled cell surface proteins were precipitated with streptavidin beads, separated by SDS-PAGE, followed by Western blotting with anti-*myc* antibody (1:100). b, total cell expression of hOAT1 Wt and its mutant L503A/L504A. Cells were lysed, and their proteins were separated by SDS-PAGE, followed by Western blotting with anti-*myc* antibody. Mature form was shown as arrow, and immature form was shown as arrowhead.

understanding in individual difference in drug response related to potential genetic variation.

In the current studies, we used alanine-scanning mutagenesis to examine the functional importance of each residue within TM 12 of hOAT1. Through this approach, we discovered several amino acids. Tyr-490, and a dileucine L503/L504, when substituted with alanine, had the most dramatic functional effects. However, other mutants with reduced transport activity may also be functionally important and need to be further investigated.

Tyr-490 seems to be critical for the stability of the transporter. We showed that substitution of Tyr-490 with alanine led to the dramatic loss of transport activity. To explore the underlying mechanisms for such loss of transport activity, we replaced Tyr-490 with Phe or Trp (Fig. 2). The side chain of Tyr contains an aromatic ring and a -OH group. The side chain of Phe contains only an aromatic ring, whereas the side chain of Trp contains both an aromatic ring and an indole ring. We showed that substitution of Tyr-490 with Trp, in part, recovered the transport activity lost by substitution of Tyr-490 with alanine, and substitution of Tyr-490 with Phe fully recovered the transport activity, suggesting that the aromatic ring and the size of the side chain of Tyr-490, but not its –OH group are critically involved in hOAT1 function.

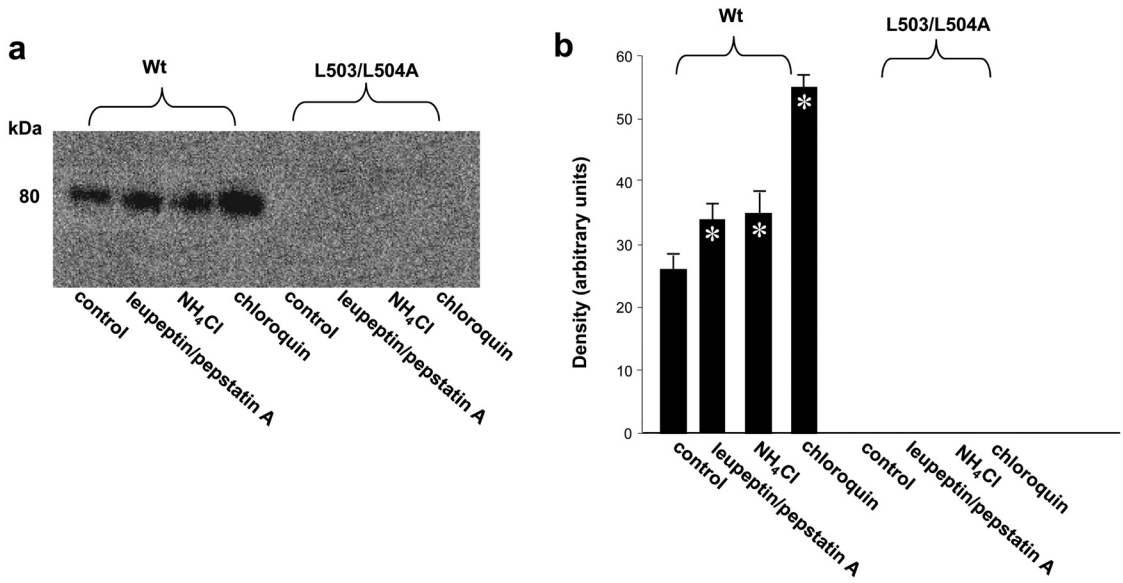

Fig. 8. The effect of lysosomal inhibitors on the expression of hOAT1 Wt and its mutant L503/L504A. a, Western blot analyses. Cells were treated for 16 h with lysosomal inhibitors leupeptin /pepstatin A (50, 100 μg/ml), NH_4Cl (2, 5, 15 mM), and chloroquin (100, 200 μM). Treated cells were lysed, followed by Western blotting with anti-*myc* antibody (1:100). The blot only showed the result with lysosomal inhibitors at the following concentrations: leupeptin/pepstatin A (50 μg/ml), NH_4Cl (2 mM), and chloroquin (100 μM). Inhibitors at other concentrations gave similar results (not shown). b, densitometry analysis of band densities from a. The results represent data from three experiments.

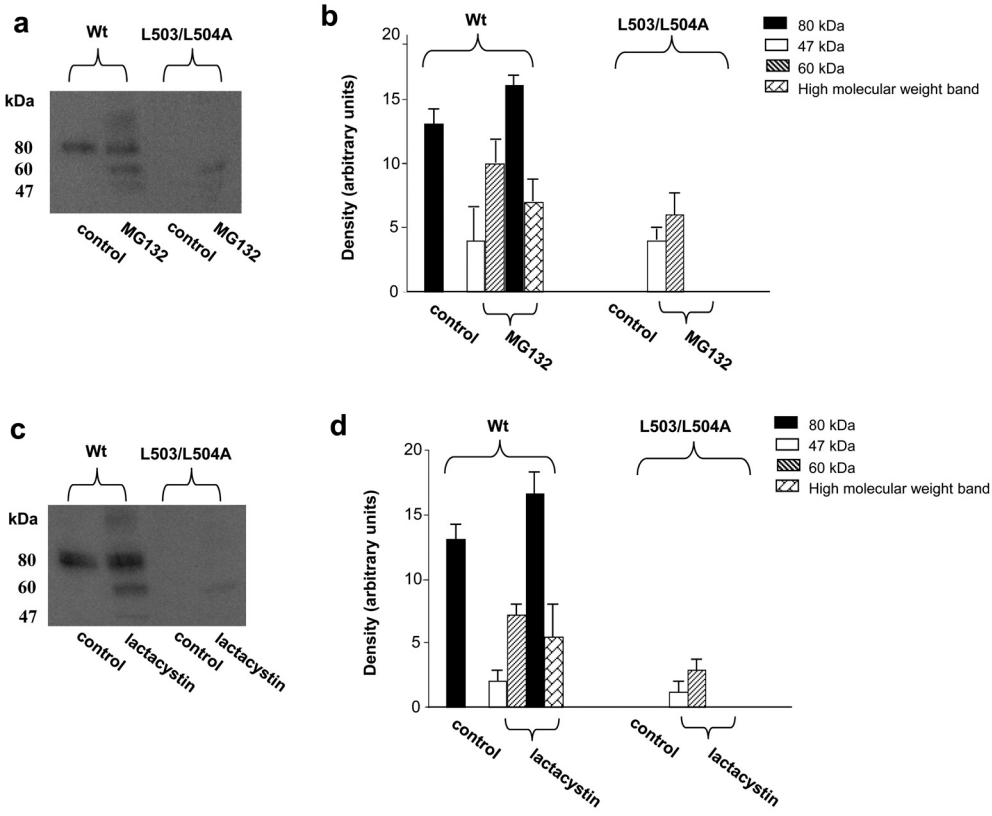

Fig. 9. The effect of proteasomal inhibitors on the expression of hOAT1 wild type (Wt) and its mutant L503/L504A. a, c, cells were treated for 6 h with proteasomal inhibitors MG132 (10 μM) (a) or lactacystin (10 μM) (c). Treated cells were lysed, followed by Western blotting using anti-*myc* antibody (1:100). b, d, densitometry analysis of band densities from a and c as well as other experiments. The results represent data from three experiments.

Our kinetic analysis showed that the reduced transport activity of Y490W was mainly due to a reduced V_{max}. We further showed that the loss of function by substitution of Tyr-490 with alanine resulted from the loss of total expression of the transporter protein (Fig. 3). By testing the effects of a battery of protease inhibitors on mutant Y490A, we observed that lysosomal inhibitors resulted in the accumulation of the mature form of the mutant transporter (Fig. 4a), and part of the accumulated mature form was able to target to the cell surface (Fig. 4c), which led to an increased transport activity (Fig. 4e). These results suggest that mutation at Tyr-490 may destabilize the transporter at the cell surface, which led to the internalization of the transporter and the subsequent degradation through the lysosomal pathway.

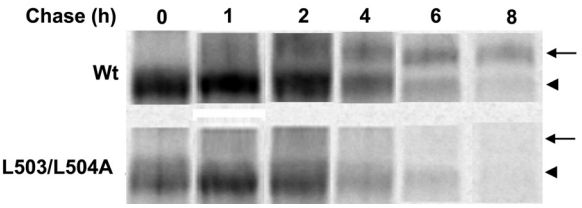

Fig. 10. Analyses of the role of dileucine L503/L504 in the maturation of hOAT1 by pulse-chase labeling. The chase began after 30 min of pulse labeling. Mature form was shown as arrow, and the immature form was shown as arrowhead.

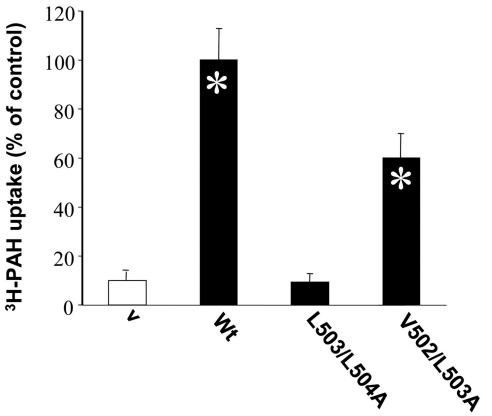

Fig. 11. PAH uptake by hOAT1 Wt and its mutants V502/L503A and L503/L504A. Transport of PAH (20 μM, 3 min) in cells expressing hOAT1 Wt and its mutants were measured. Uptake activity was expressed as a percentage of the uptake measured in Wt. The results represent data from three experiments, with triplicate measurements for each mutant. *, values significantly different ($p < 0.05$) from that of mock control (V).

Proteasomal inhibitors resulted in the accumulation of both the immature form and the mature form of the mutant transporter (Fig. 5). However, our biotinylation study showed that the mature form accumulated by protease inhibitors was not delivered to the cell surface. It is possible that the immature form accumulated by proteasomal inhibitors escaped from the ER quality control and was further processed to mature form with a defective conformation, which was unable to adhere to the cell surface. It is also possible that the protease inhibitors affect the expression/function of hOAT1-interacting proteins that prevent mature hOAT1 from inserting into the plasma membrane.

Our conclusion that Tyr-490 is critical for the stability of the transporter was further reinforced by our pulse-chase studies (Fig. 6). We showed that hOAT1 mutant Y490A matured as efficiently as that of hOAT1 wild type. Therefore, Tyr-490 does not seem to play a role in the maturation efficiency of the transporter.

In contrast to Tyr-490, mutation of which caused an accelerated degradation of the transporter, mutation at L503/L504 seems to mainly prevent the maturation of the transporter (Fig. 10), although certain role of L503/L504 in stabilizing the transporter may also be possible because the treatment of L503/L504A-expressing cells with proteasome inhibitors slightly increased the expression of a band centered around 60 kDa (Fig. 9). The specific role of L503/L504 in the maturation of hOAT1 was further reinforced by our demonstration that, when Leu-503 was simultaneously mutated with another adjacent residue Val-502 instead of Leu-504, the double mutant V502A/L503A exhibited significant transport activity (Fig. 11), indicating that this mutant is capable to produce a fully glycosylated cell surface form of the transporter. Therefore, it is the alteration of a specific dileucine rather than the simultaneous alteration of two amino acids at a specific location of the TM 12 that impairs the maturation. Dileucine mutation may impose a folding defect on hOAT1, which is recognized by the ER quality control machinery as non-native and therefore marked for degradation by proteasome. As a result, escape from the ER for maturation is severely compromised.

In summary, our current studies are the first to highlight the central role of the TM 12 of hOAT1: Tyr-490 is essential in maintaining the stability of the transporter, and dileucine L303/L304 is critically involved both in correct folding of the transporter, which is required for the maturation of the transporter, and in maintaining the stability of the transporter. We have previously demonstrated that hOAT1 function could be disrupted by impaired cell surface targeting or impaired substrate recognition (Hong et al., 2004; Tanaka et al., 2004; Zhou et al., 2005). The current studies demonstrated that hOAT1 dysfunction could be determined within TM 12 by the accelerated degradation and defective maturation of the transporter.

Acknowledgments

We thank Weinan Du for assistance in constructing mutant transporters and Wen Xu for assistance with the pulse-chase experiments.

References

Abramson J, Smirnova I, Kasho V, Verner G, Kaback HR, and Iwata S (2003) Structure and mechanism of the lactose permease of Escherichia coli. *Science* **301:**610–615.

Anzai N, Kanai Y, and Endou H (2006) Organic anion transporter family: current knowledge. *J Pharmacol Sci* **100:**411–426.

Bahn A, Ebbinghaus C, Ebbinghaus D, Ponimaskin EG, Fuzesï L, Burckhardt G, and Hagos Y (2004) Expression studies and functional characterization of renal human organic anion transporter 1 isoforms. *Drug Metab Dispos* **32:**424–430.

Bahn A, Hagos Y, Reuter S, Balen D, Brzica H, Krick W, Burckhardt BC, Sabolic I, and Burckhardt G (2008) Identification of a new urate and high affinity nicotinate transporter, hOAT10 (SLC22A13). *J Biol Chem* **283:**16332–16341.

Bauman PA and Blakely RD (2002) Determinants within the C-terminus of the human norepinephrine transporter dictate transporter trafficking, stability, and activity. *Arch Biochem Biophys* **404:**80–91.

Bello V, Goding JW, Greengrass V, Sali A, Dubljevic V, Lenoir C, Trugnan G, and Maurice M (2001) Characterization of a di-leucine-based signal in the cytoplasmic tail of the nucleotide-pyrophosphatase NPP1 that mediates basolateral targeting but not endocytosis. *Mol Biol Cell* **12:**3004–3015.

Cha SH, Sekine T, Kusuhara H, Yu E, Kim JY, Kim DK, Sugiyama Y, Kanai Y, and Endou H (2000) Molecular cloning and characterization of multispecific organic anion transporter 4 expressed in the placenta. *J Biol Chem* **275:**4507–4512.

Eckhardt ER, Cai L, Shetty S, Zhao Z, Szanto A, Webb NR, and Van der Westhuyzen DR (2006) High density lipoprotein endocytosis by scavenger receptor SR-BII is clathrin-dependent and requires a carboxyl-terminal dileucine motif. *J Biol Chem* **281:**4348–4353.

El-Sheikh AA, Masereeuw R, and Russel FG (2008) Mechanisms of renal anionic drug transport. *Eur J Pharmacol* **585:**245–255.

Hong M, Zhou F, and You G (2004) Critical amino acid residues in transmembrane domain 1 of the human organic anion transporter hOAT1. *J Biol Chem* **279:**31478–31482.

Huang Y, Lemieux MJ, Song J, Auer M, and Wang DN (2003) Structure and mechanism of the glycerol-3-phosphate transporter from Escherichia coli. *Science* **301:**616–620.

Jensen TJ, Loo MA, Pind S, Williams DB, Goldberg AL, and Riordan JR (1995) Multiple proteolytic systems, including the proteasome, contribute to CFTR processing. *Cell* **83:**129–135.

Kopito RR (1997) ER quality control: the cytoplasmic connection. *Cell* **88:**427–430.

Kusuhara H, Sekine T, Utsunomiya-Tate N, Tsuda M, Kojima R, Cha SH, Sugiyama Y, Kanai Y, and Endou H (1999) Molecular cloning and characterization of a new multispecific organic anion transporter from rat brain. *J Biol Chem* **274:**13675–13680.

Peña-Münzenmayer G, Catalán M, Cornejo I, Figueroa CD, Melvin JE, Niemeyer MI, Cid LP, and Sepúlveda FV (2005) Basolateral localization of native ClC-2 chloride channels in absorptive intestinal epithelial cells and basolateral sorting encoded by a CBS-2 domain di-leucine motif. *J Cell Sci* **118:**4243–4252.

Perry JL, Dembla-Rajpal N, Hall LA, and Pritchard JB (2006) A three-dimensional

model of human organic anion transporter 1: aromatic amino acids required for substrate transport. *J Biol Chem* **281:**38071–38079.
Popp C, Gorboulev V, Müller TD, Gorbunov D, Shatskaya N, and Koepsell H (2005) Amino acids critical for substrate affinity of rat organic cation transporter 1 line the substrate binding region in a model derived from the tertiary structure of lactose permease. *Mol Pharmacol* **67:**1600–1611.
Schnabolk GW, Youngblood GL, and Sweet DH (2006) Transport of estrone sulfate by the novel organic anion transporter Oat6 (Slc22a20). *Am J Physiol Renal Physiol* **291:**F314–F321.
Sekine T, Cha SH, Tsuda M, Apiwattanakul N, Nakajima N, Kanai Y, and Endou H (1998) Identification of multispecific organic anion transporter 2 expressed predominantly in the liver. *FEBS Lett* **429:**179–182.
Sekine T, Watanabe N, Hosoyamada M, Kanai Y, and Endou H (1997) Expression cloning and characterization of a novel multispecific organic anion transporter. *J Biol Chem* **272:**18526–18529.
Sepp-Lorenzino L, Ma Z, Lebwohl DE, Vinitsky A, and Rosen N (1995) Herbimycin A induces the 20 S proteasome- and ubiquitin-dependent degradation of receptor tyrosine kinases. *J Biol Chem* **270:**16580–16587.
Shin HJ, Anzai N, Enomoto A, He X, Kim do K, Endou H, and Kanai Y (2007) Novel liver-specific organic anion transporter OAT7 that operates the exchange of sulfate conjugates for short chain fatty acid butyrate. *Hepatology* **45:**1046–1055.
Srimaroeng C, Perry JL, and Pritchard JB (2008) Physiology, structure, and regulation of the cloned organic anion transporters. *Xenobiotica* **38:**889–935.
Sweet DH, Wolff NA, and Pritchard JB (1997) Expression cloning and characterization of ROAT1. The basolateral organic anion transporter in rat kidney. *J Biol Chem* **272:**30088–30095.
Tanaka K, Xu W, Zhou F, and You G (2004) Role of glycosylation in the organic anion transporter OAT1. *J Biol Chem* **279:**14961–14966.
Ward CL, Omura S, and Kopito RR (1995) Degradation of CFTR by the ubiquitin-proteasome pathway. *Cell* **83:**121–127.
Yokoyama H, Anzai N, Ljubojevic M, Ohtsu N, Sakata T, Miyazaki H, Nonoguchi H, Islam R, Onozato M, Tojo A, et al. (2008) Functional and immunochemical characterization of a novel organic anion transporter Oat8 (Slc22a9) in rat renal collecting duct. *Cell Physiol Biochem* **21:**269–278.
You G (2004) The role of organic ion transporters in drug disposition: an update. *Curr Drug Metab* **5:**55–62.
Youngblood GL and Sweet DH (2004) Identification and functional assessment of the novel murine organic anion transporter Oat5 (Slc22a19) expressed in kidney. *Am J Physiol Renal Physiol* **287:**F236–F244.
Zhang X, Shirahatti NV, Mahadevan D, and Wright SH (2005) A conserved glutamate residue in transmembrane helix 10 influences substrate specificity of rabbit OCT2 (SLC22A2). *J Biol Chem* **280:**34813–34822.
Zhou F, Xu W, Hong M, Pan Z, Sinko PJ, Ma J, and You G (2005) The role of N-linked glycosylation in protein folding, membrane targeting, and substrate binding of human organic anion transporter hOAT4. *Mol Pharmacol* **67:**868–876.

Address correspondence to: Dr. Guofeng You, Dept. of Pharmaceutics, Rutgers, The State University of New Jersey, 160 Frelinghuysen Road, Piscataway, NJ 08854. E-mail: gyou@rci.rutgers.edu